

Isolation and Functional Analysis of Two Gibberellin 20-Oxidase Genes from Satsuma Mandarin (*Citrus unshiu* Marc.)

Nobuhiro Kotoda^{1,2*}, Satoshi Matsuo³, Ichiro Honda⁴, Kanako Yano¹ and Tokurou Shimizu¹

¹NARO Institute of Fruit Tree Science, Shizuoka 424-0292, Japan

²Faculty of Agriculture, Saga University, Saga 840-8502, Japan

³NARO Institute of Vegetable and Tea Science, Tsu 514-2392, Japan

⁴Department of Biotechnology, Maebashi Institute of Technology, Maebashi 371-0816, Japan

Satsuma mandarin (*Citrus unshiu* Marc.) has two GA 20-oxidase genes, *CuGA20ox1* and *CuGA20ox2*, and the genomic sequence for *CuGA20ox1* is shorter than that for *CuGA20ox2*, although the coding region of cDNA for *CuGA20ox1* is slightly longer than that for *CuGA20ox2*. Southern blot analysis revealed that 12 *Citrus* cultivars examined and trifoliolate orange [*Poncirus trifoliata* (L.) Raf.] have at least two types of GA 20-oxidase genes, such as *CuGA20ox1* and *CuGA20ox2* genes. *CuGA20ox1* and *CuGA20ox2* were differentially expressed in various tissues. *CuGA20ox1* was expressed in almost all of the tissues investigated with relatively higher expression in vegetative than in reproductive tissues, whereas *CuGA20ox2* was specifically expressed in flower buds just before anthesis. These distinct expression patterns of *CuGA20ox1* and *CuGA20ox2* imply that function of these two genes diverged in the process of evolution. The specific and relatively higher expression of *CuGA20ox2* in flower buds would explain why GA-like activity was higher in Satsuma mandarin's ovaries at anthesis. Transgenic *Arabidopsis* [*Arabidopsis thaliana* (L.) Heynh] plants ectopically expressing *CuGA20ox1* or *CuGA20ox2* were examined to elucidate the function of these two Satsuma mandarin genes. Phenotypic analysis revealed that both *CuGA20ox1* and *CuGA20ox2* caused elongated inflorescence but did not affect the timing of flowering in transgenic *Arabidopsis* as compared with wild-type controls. Ectopic expression of *CuGA20ox1* and *CuGA20ox2* significantly affected the levels of GA₂₄ and GA₃₄ on the non-13-hydroxylation pathway; GA₂₄ decreased and GA₃₄ increased. This observation indicates that both *CuGA20ox1* and *CuGA20ox2* accelerated the conversion of GA₂₄, a substrate of a GA 20-oxidase, to GA₉, a precursor of an active form of GA₄. Likewise, on the early-13-hydroxylation pathway, ectopic expression of *CuGA20ox1* significantly decreased GA₁₉ and increased GA₂₉ and GA₈, inactive metabolites of 2-hydroxylation of GA₂₀ and GA₁, respectively, suggesting the activation of this biosynthetic pathway. *CuGA20ox2* also had a tendency to activate the early-13-hydroxylation pathway although it increased only GA₂₀ with a statistically significant difference. Taken together, we concluded that *CuGA20ox1* and/or *CuGA20ox2* activated both the early-13- and non-13-hydroxylation pathways for increasing active GAs, resulting in elongated inflorescences in transgenic *Arabidopsis*.

Key Words: *CuGA20ox1*, *CuGA20ox2*, LC-MS/MS, plant growth substances, seedless fruit.

Introduction

Gibberellins (GAs) are plant growth substances, orig-

inally identified in a rice bakanae fungus [*Gibberella fujikuroi* (Sawada) Wollenw.] as a toxin that caused rice to elongate, resulting in lodging and low yields (Kurosawa, 1926; Yabuta and Sumiki, 1938). In the late 1950s, the chemical structure of GA₃ was determined (Cross, 1960; Cross et al., 1959; Takahashi et al., 1961) and total synthesis of some GAs was achieved in the 1960s to 1970s (Corey et al., 1978; Mori et al., 1969), consequently leading to their use in biochemical studies and agricultural practices. Kawarada and Sumiki (1959) reported that Satsuma mandarin (*Citrus unshiu* Marc.)

Received; June 4, 2015. Accepted; September 23, 2015.

First Published Online in J-STAGE on November 28, 2015.

This study was supported by a Grant-in-Aid for scientific research from the Ministry of Education, Culture, Sports, Science and Technology (No. 24580058) and a Research Project for Molecular Evaluation of Parthenocarpy on Horticultural Crops from NARO.

* Corresponding author (E-mail: koto@cc.saga-u.ac.jp; nobu_fruits@yahoo.co.jp).

contained GA₁ in its water sprouts (vegetative shoots that produce neither flowers nor fruit), and first demonstrated the existence of a GA in woody plants.

Extensive studies for many years revealed that GAs are involved in a wide variety of physiological events, such as cell elongation, cell division, dormancy, flowering, and fruit development in higher plants. Many researchers have also conducted biochemical studies to clarify the biosynthetic pathway of GAs in plants (for reviews: Hedden and Kamiya, 1997; Hedden and Phillips, 2000; Yamaguchi, 2008). These studies revealed that there are two pathways for synthesizing active GAs; the pathway where GAs, such as GA₁ and GA₃, are synthesized sequentially through GA₅₃, GA₄₄, GA₁₉, and GA₂₀ after the synthesis of GA₁₂ through some steps from isopentenyl diphosphate and dimethylallyl diphosphate, and another pathway where GAs, such as GA₄, are synthesized through GA₁₅, GA₂₄, and GA₉ after the synthesis of GA₁₂ (Fig. 1). The former and the latter pathways are known as the early-13-hydroxylation and the non-13-hydroxylation pathways, respectively, because GAs in the former pathway are hydroxylated at position C13 in the early step from GA₁₂ to GA₅₃, whereas those in the latter are not. As in rice, citrus, such as Satsuma mandarin, is considered to use the early-13-hydroxylation pathway because citrus accumulates 13-OH GAs, such as GA₁, more abundantly than it accumulates 13-H GAs, such as GA₄ (Goto et al., 1989; Poling and Maier, 1988; Talon et al., 1990a, b; Turnbull, 1989). Recently, the genes encoding the enzyme to catalyze the step from GA₁₂ to GA₅₃, which have been unknown for many years, were identified as *CYP714B1* and *CYP714B2* in rice (*Oryza sativa*

L.) (Magome et al., 2013). In the rice double mutant, *cyp714b1 cyp714b2*, the concentration of 13-H GAs that include GA₄ increased, on the other hand, transgenic rice overexpressing *CYP714B1* or *CYP714B2* increased the level of 13-OH GAs that include GA₁, which show semi-dwarfism. This result suggests that these GA 13-oxidases may be involved in the switching of the two biosynthetic pathways that diverge after GA₁₂.

Also in woody plants like fruit trees, much effort has been devoted to understanding the role of GAs. It has been demonstrated, for example, that in apple (*Malus domestica* Borkh.) and citrus GAs function negatively to flower induction (Luckwill and Silva, 1979; Monselise, 1979; Tromp, 1982). On the other hand, it is reported that GAs play a positive role in the flowering of Japanese cedar (*Cryptomeria japonica*), although the mechanism underlying the phenomenon remains to be clarified (Nagao et al., 1989). The method for producing seedless grapes by applying GA₃ was established as early as the structure of GA₃ was determined in the late 1950s. Kishi and Tasaki (1960) found that berries matured early and were seedless when their flower buds were treated with adequate concentrations of GA₃ about three weeks before full bloom in ‘Delaware’ grape, which was originally a seeded cultivar. These findings were applied commercially to the culture of seedless grapes in Japan for the first time in the world.

Production of seedless fruit is very important for breeders and growers to meet consumer demands in citriculture as well as in viticulture. Satsuma mandarin is considered absolutely seedless because it is female and male sterile in addition to parthenocarpic and very

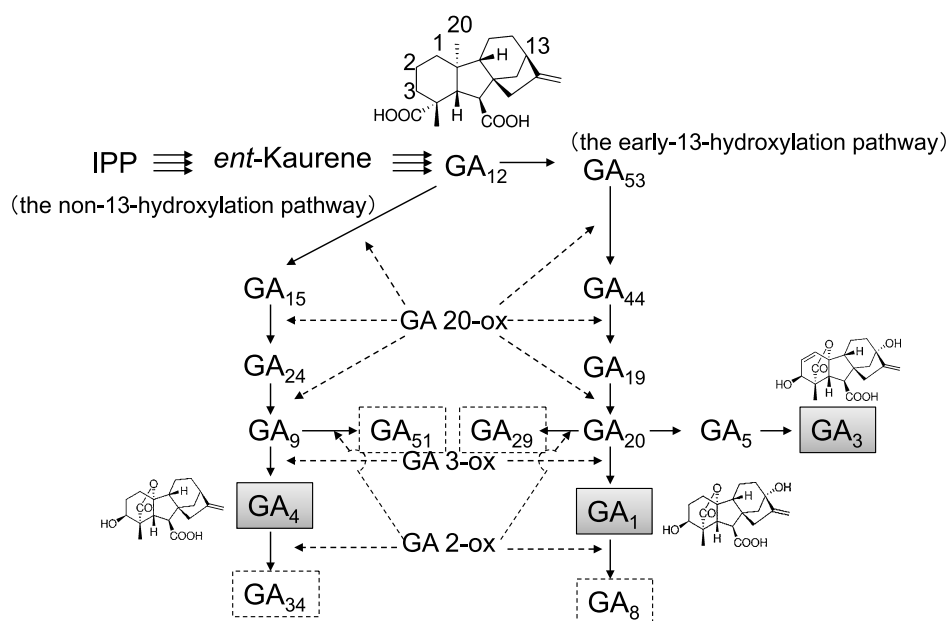


Fig. 1. Biosynthetic pathway of gibberellin in higher plants. IPP, isopentenyl diphosphate, GA20-ox, GA 20-oxidase; GA3-ox, GA 3-oxidase; GA2-ox, GA 2-oxidase. Boxes in gray represent active GAs and dotted boxes represent inactive GAs.

productive without pollinators (Iwamasa, 1966; Vardi et al., 2008). Talon et al. (1990b) reported that in Satsuma mandarin the development of ovaries preceded that in Clementine (*Citrus clementina* hort. ex Tanaka), which shows self-incompatibility and low parthenocarpy. In addition, active GAs and its precursors, such as GA₁₉, GA₂₀, and GA₁, were more highly accumulated in the ovaries at around anthesis in Satsuma mandarin than in Clementine (Talon et al., 1990b, 1992). These results imply a relationship between the degree of early fruit (ovary) development and parthenocarpy and the endogenous GAs there. In recent years, genes related to GA biosynthesis have been isolated and analyzed to clarify their functions in citrus (Fagoaga et al., 2007; Huerta et al., 2009; Vidal et al., 2001, 2003). Fagoaga et al. (2007) demonstrated that transgenic Carrizo citrange [a hybrid of trifoliate orange and sweet orange (*Citrus sinensis* Osbeck)] that overexpressed *CcGA20ox1* (a Carrizo citrange GA 20-oxidase gene) increased the GA₁ level and the height of the plant. In addition, Huerta et al. (2009) identified and characterized the second citrus GA 20-oxidase gene, *CcGA20ox2*, in Carrizo citrange. In this study, we report the characterization of two GA 20-oxidase genes from Satsuma mandarin, which is cultivated in the largest area in the citriculture of Japan, as a first step in clarifying the roles of these genes and the distribution of GAs in the life cycle of citrus, such as Satsuma mandarin. Satsuma mandarin originated in Japan, and is a unique and important scion cultivar providing us with seedless and easy-peeling fruit with health functional ingredients for over 150 years. Molecular characterization of GA biosynthetic genes including *Citrus unshiu* GA-20 oxidase genes would be helpful to studying the mechanisms of parthenocarpy and peel puffins in the future.

Materials and Methods

Plant materials

Tissue samples of a Satsuma mandarin (*Citrus unshiu* Marc.) cultivar (cv.) 'Silverhill' in the adult phase (age: 43 yr) were collected from the experimental field at the NARO Institute of Fruit Tree Science in Okitsu, Shizuoka, Japan. Two-year-old nucellar seedlings of 'Silverhill', which were distinguished from hybrids by simple sequence repeat (SSR) genotyping analysis, were used for expression analysis in the juvenile phase. Satsuma mandarins (cvs. 'Silverhill' and 'Miyagawawase'), 'Kiyomi' tangor (*C. unshiu* × *C. sinensis* Osbeck), Hyuganatsu (*C. tamurana* hort. ex Tanaka), Clementine, 'Clementine Vita' (*Citrus clementina* hort. ex Tanaka cv. 'Clementine Vita'), sweet orange (*C. sinensis* Osbeck cv. 'Trovita'), pummelo (*C. grandis* Osbeck cvs. 'Benimadoka' and 'Banpeiyu'), Sudachi (*C. sudachi* hort. ex Shirai), Yuzu (*C. junos* Sieb. ex Tanaka), Kunenbo (*C. nobilis* Lour.), and trifoliate orange [*Poncirus trifoliata* (L.) Raf.] were used for

Southern blot analysis. Wild-type plants of ecotype Columbia (Col) were used for *Arabidopsis* [*Arabidopsis thaliana* (L.) Heynh] transformation.

Isolation of *CuGA20ox1* and *CuGA20ox2* genes from *Satsuma mandarin*

Leaves and ovaries of Satsuma mandarin 'Silverhill' were used to isolate the cDNA of GA 20-oxidase genes *CuGA20ox1* and *CuGA20ox2*, respectively. cDNA from the leaves and ovaries was amplified by polymerase chain reaction (PCR) with the primers CcGA20ox1(-24 > -3) and CcGA20ox1(1239 < 1258) for *CuGA20ox1* and CcGA20ox2(-29 > -4) and CcGA20ox2(1124 < 1147) for *CuGA20ox2*, designed based on the sequences of *CcGA20ox1* (AJ250187; Vidal et al., 2001) and *CcGA20ox2* (EU834066; Huerta et al., 2009), respectively, using KOD-plus (Toyobo, Osaka, Japan). Each amplified product was cloned into a pT7Blue T-vector (Merck Millipore, Darmstadt, Germany) or a pGEM-T Easy vector (Promega, Madison, WI, USA) after an adenine nucleotide addition to the products. To obtain genomic DNA of *CuGA20ox1* and *CuGA20ox2*, the same primer sets as those for cDNA isolation were used with the total DNA of Satsuma mandarin 'Silverhill' as a template. All PCR products for the isolation of cDNA and genomic DNA of *CuGA20ox1* and *CuGA20ox2* were subcloned and sequenced (ABI 3130xl DNA sequencer; Life Technologies, Carlsbad, CA, USA). The primer sets used in gene cloning are listed in Table 1.

Construction of a phylogenetic tree

Amino acid sequences were analyzed using the ClustalX multiple sequence alignment program ver. 1.83 (Jeanmougin et al., 1998) and BioEdit ver. 7.7.0 (Hall, <http://www.mbio.ncsu.edu/BioEdit/bioedit.html>). The tree was constructed by the neighbor-joining (N-J) method for the deduced amino acid sequence of the GA 20-oxidase genes from apple [*MdGA20ox* (AB037114), *MdGA20ox* (MDP0000136940)], *Arabidopsis* [*AtGA20ox1* (AT4G25420), *AtGA20ox2* (AT5G51810), *AtGA20ox3* (AT5G07200), *AtGA20ox4* (AT1G60980), *AtGA20ox5* (AT1G44090A)], Carrizo citrange [*Citrus sinensis* × *Poncirus trifoliata*, *CcGA20ox1* (AJ250187), *CcGA20ox2* (EU834068)], Clementine [*CclGA20ox1* (Ciclev10005157m), *CclGA20ox2* (Ciclev10020694m)], common bean [*Phaseolus vulgaris* L., *PvGA20ox* (U70530, U70531, U70532)], European beech [*Fagus sylvatica* L., *FsGA20ox1* (AJ420192)], grape [*Vitis vinifera* L., *VvGA20ox* (DQ508817)], lettuce [*Lactuca sativa*, *LsGA20ox1* (AB012203), *LsGA20ox2* (AB012204), *LsGA20ox3* (AB031202)], morning glory [*Ipomoea nil* (L.) Roth, *InGA20ox1* (AB099488), *InGA20ox2* (AB099489)], pea [*Pisum sativum* L., *PsGA20ox* (U70471), *PsGA20ox* (U58830)], *Physcomitrella patens* (Hedw.)

Table 1. Primer sets used in gene cloning, probe labelling, quantitative real-time RT-PCR analysis, and vector construction.

Primers	Oligonucleotide (5' → 3')
<u>Gene cloning</u>	
CcGA20ox1(−24>−3)	CTC AAC TCA CAA CTC TTT AAT G
CcGA20ox1(1239<1258)	TTG CTA GCC CTT TGT CTT CC
CcGA20ox2(−29>−4)	ACC CAT CTA TCT ATT ACA ATC TAT CT
CcGA20ox2(1124<1147)	CAT CAT CTT AAA TTT CCT ATT CAC
<u>Probe labelling</u>	
CcGA20ox1(−24>−3)	CTC AAC TCA CAA CTC TTT AAT G
CcGA20ox1(1239<1258)	TTG CTA GCC CTT TGT CTT CC
CuGA20ox2(1 > 26)	ATG TCA ATG GAT TGT TAC AAT TCA AG
CuGA20ox2(1096 < 1119)	TTA AAT ATT GAC ATG CTG TTG AAG
<u>Real-time RT-PCR</u>	
CuGA20ox1(522>543)	GCT TAA CAC AAT GGG AGA TGA A
CuGA20ox1(627<646)	CCC TGT CTA CAC CAA GAC TT
CuGA20ox2(481>505)	GTC GAA GAT TAT TTC TTC AAC GTA A
CuGA20ox2(578<600)	CAT TCC TAA CAG CTC CAT GAT CC
CuActin(−86>−66)	GAG CGA TAG AGA GAA TCG ACA
CuActin(−1 < 19)	TAT CCT CAG CAT CGG CCA TT
AtTUB4-F	TTC ATA TCC AAG GCG GTC AAT GTG G
AtTUB4-R	CGA GCT TGA GGG TAC GGA AAC AG
<u>Vector construction</u>	
CuGA20ox1(1 < 20)XbaI	AAt cta gaA TGG CAA TAG ACT GCA TAA A
CuGA20ox1(1131 < 1152)SacI	AAg agc tcT CAT TTC AGC TGT TTT TTC TGT
CuGA20ox2(1 > 25)XbaI	AAt cta gaA TGT CAA TGG ATT GTT ACA ATT CAA
CuGA20ox2(1095 < 1119)SacI	AAg agc tcT TAA ATA TTG ACA TGC TGT TGA AGC

The thermal cycle programs for real-time RT-PCR were as follows: 95°C for 10 min, followed by 40 cycles of at 95°C for 15 s, 60°C for 60 s for *CuGA20ox1* [CuGA20ox1(522 > 543) and CuGA20ox1(627 < 646)], *CuGA20ox2* [CuGA20ox2(481 > 505) and CuGA20ox2(578 < 600)], *CuActin* [CuActin(−86 > −66) and CuActin(−1 < 19)] and AtTUB4 (AtTUB4-F and AtTUB4-R). Characters in lowercase indicate the site for restriction enzymes used for vector construction.

Bruch & Schimp [*PpGA20ox* (EU262757)], poplar [*Populus nigra* L., *PnGA20ox1* (AB089675); *P. Alba* L., *PaGA20ox1a* (AB090238); *P. tremula* × *P. tremuloides* Michx., *PtPtGA20ox1* (AJ001326)], potato [*Solanum tuberosum* L., *StGA20ox1* (AJ291453), *StGA20ox2* (AJ291454)], *Selaginella moellendorffii* [*SmGA20ox* (EU262754)], rice [*Oryza sativa* L., *OsGA20ox1* (U50333), *OsGA20ox2* (AB469066)], Satsuma mandarin [*CuGA20ox1* (LC056054), *CuGA20ox2* (LC056055)], spinach [*Spinacia oleracea* L., *SoGA20ox* (U33330)], sweet orange [*Citrus sinensis*, *CsGA20ox1* (orange1.1g016776m), *CsGA20ox2* (orange1.1g041132m)], tobacco [*Nicotiana tabacum* L., *NtGA20ox* (AB012856); *N. glauca* L., *NsGA20ox2* (AF494088)], and tomato [*Solanum lycopersicum* L., *LeGA20ox1* (AF049898), *LeGA20ox2* (AF049899), *LeGA20ox3* (AF049900), *SlGA20ox4* (EU675630)]. The phylogenetic tree was displayed using the N-J plot unrooted (Perrière and Gouy, 1996) with bootstrap values for 1000 resamplings in each branch.

DNA extraction and hybridization analysis

Genomic DNA was isolated using a cetyltrimethylammonium bromide (CTAB)-based method as de-

scribed in Kotoda et al. (2002). For Southern blot analysis, the genomic DNA (5 µg) was digested with *XbaI*, electrophoresed on a 0.8% agarose gel, and then blotted onto Hybond-N+ nylon membranes (GE Healthcare Bio-Sciences Corp., Piscataway, NJ, USA). The blotted membrane was hybridized with digoxigenin (DIG; Roche Diagnostics, Mannheim, Germany)-labeled *CuGA20ox1* or *CuGA20ox2* cDNA, which was amplified by PCR with a pair of primers used for gene cloning for *CuGA20ox1* and with a pair of primers CuGA20ox2(1 > 26) and CuGA20ox2(1096 < 1119) for *CuGA20ox2* and a DIG mixture (Roche Diagnostics). Hybridization was performed in DIG Easy Hyb (Roche Diagnostics) at 42°C for 16 h, followed by two rinses in 2x SSC containing 0.1% (w/v) SDS at room temperature for 2 min and two washes in 0.5x SSC containing 0.1% (w/v) SDS at 68°C for 20 min as described by Kotoda et al. (2006). Detection was performed according to the manufacturer's protocol (Roche Diagnostics). Chemiluminescent signals were visualized using the NightOWL image analyzer (Berthold Technologies, Bad Wildbad, Germany). The primer sets used for labelling are listed in Table 1.

Expression analysis by quantitative real-time RT-PCR

Using a phenol-SDS based method as described by Ikoma et al. (1996), total RNA was extracted for analysis from seeds, roots (whole roots including lateral ones), stems, new and old leaves, and nodes of two-year-old juvenile nucellar seedlings as well as from new and old leaves, shoot apices in August, flower buds (just before anthesis), young fruit in June, juice sacs (in September, November, and December), and peels (in September and December) of adult 'Silverhill' Satsuma mandarin trees. For transgene expression analysis, whole plants of transformants in second generation (T_2) and controls were collected two months after incubation, and total RNA was extracted from two individuals per each line by using a CTAB based methods. The samples of total RNA were then purified using an RNeasy Mini Kit (Qiagen GmbH, Hilden, Germany). First-strand cDNA was synthesized from 1 μ g of total RNA in 20 μ L of a reaction mixture using a QuantiTect Reverse Transcription Kit (Qiagen). Subsequent PCR reactions were performed with 1 μ L of the first-strand cDNA as a template in a total volume of 12.5 μ L using the ABI PRISM[®] 7000 (Applied Biosystems, Foster City, CA, USA). Transcripts of *CuGA20ox1*, *CuGA20ox2*, an actin gene derived from Satsuma mandarin (*CuActin*; for reference, Phytozome Transcript Name Ciclev10025866m), and an *Arabidopsis* β tubulin gene (*AtTUB4*) were identified with the specific primers. The primer sets used in the quantitative real-time RT-PCR (qRT-PCR) analysis and the PCR conditions are described in Table 1. A citrus *CuActin* gene and an *Arabidopsis AtTUB* gene were used as an internal control for analyzing Satsuma mandarin and *Arabidopsis*, respectively. qRT-PCR was performed three times, and transcript levels were normalized against each internal control.

Construction of the transformation vector

To construct a vector for the constitutive expression of *CuGA20ox1* and *CuGA20ox2*, the coding region of each gene was amplified by PCR with pairs of primers *CuGA20ox1*(1 < 20)*Xba*I and *CuGA20ox1*(1131 < 1152)*Sac*I for *CuGA20ox1*, and with a pair of primers *CuGA20ox2*(1 > 25)*Xba*I and *CuGA20ox1*(1095 < 1119)*Sac*I for *CuGA20ox2*. An amplified PCR product was subsequently digested with *Xba*I and *Sac*I, and then cloned into the *Xba*I/*Sac*I sites of the modified pSMAK193E (35S Ω ::pSMAK193E; described in Kotoda et al., 2010), a kanamycin-resistant binary vector, to be placed between the 35S Ω and 3' regions of the *Arabidopsis rbcS-2B* gene (*TrbcS*).

Arabidopsis transformation

Agrobacterium tumefaciens strain EHA101 harboring a binary vector with 35S Ω ::*CuGA20ox1* or 35S Ω ::*CuGA20ox2* was used to transform *Arabidopsis thaliana* (Col) plants using the floral-dip method

(Clough and Bent, 1998). After two to five adult leaves had developed, kanamycin-resistant transformants were transplanted from the plate to moistened potting soil composed of vermiculite and grown in a growth chamber (Biotron; Nippon Medical and Chemical Instruments Co., Ltd., Tokyo, Japan) set at 22°C under LD conditions (16-h photoperiod; cool white fluorescent light, 50 μ mol·m⁻²·s⁻¹). Morphological and expression analyses and quantification of gibberellins (GAs) were performed on the second generation (T_2). For morphological analysis, numbers of rosette and cauline leaves were counted on the day floral organs became visible. Numbers of inflorescences merging from the base were counted and length of 1st inflorescences (infl.) was measured one month after incubation. Whole plants of transformants (T_2) and controls were collected two months after incubation for qRT-PCR analysis described above and quantification of gibberellins (GAs) described below.

Quantitative analysis of gibberellins

Two month after the start of incubation, whole transgenic and wild-type *Arabidopsis* plants were used for the quantification of 13 gibberellins on both the early-13-hydroxylation pathway (GA₅₃, GA₄₄, GA₁₉, GA₂₀, GA₁, GA₈, and GA₂₉) and the non-13-hydroxylation pathway (GA₁₅, GA₂₄, GA₉, GA₄, GA₃₄, and GA₅₁). Five plants (about 0.4–1.2 g in total) per each transgenic line or control were collected and frozen in liquid nitrogen. These plants were then ground with a pestle in liquid nitrogen and homogenated in 80% methanol, followed by the addition of [17, 17-²H₂] GAs (5 ng each) as internal standards. A total of ten samples (one sample per each independent line of 35S Ω ::*CuGA20ox1* or 35S Ω ::*CuGA20ox2*) were prepared in this experiment (n = 5, five biological replicates). After incubation for 12 h at 4°C, each homogenate was centrifuged and supernatant was concentrated by evaporating the methanol. The concentrate was partitioned against an equal volume of *n*-hexane, and the aqueous layer was obtained, the pH of which was adjusted to 3.0. The aqueous layer was partitioned with ethyl acetate and the organic layer was obtained (three times). Then, the organic solvent was extracted three times with potassium phosphate buffer (pH = 8.3). The pH of the aqueous extracts was adjusted to/below 3.0 again, and the extracts were partitioned with ethyl acetate; then, an organic layer was obtained, followed by drying with sodium sulfate. The dried organic solvent was concentrated to evaporate the ethyl acetate after filtration through a Bond Elut[®] Reservoir (Varian, Lake Forest, CA, USA). The sample dissolved in methanol was loaded onto a reverse phase cartridge (Oasis[®] HLB, 60 mg; Waters, Milford, MA, USA) and eluted with 80% methanol. The elute was dried and then the sample in methanol was loaded onto an ion-change column (Bond Elut[®] DEA; Varian). GAs were eluted three

times with 2 mL of methanol containing 2% acetic acid, and the elute was dried, dissolved in chloroform:ethyl acetate = 1:1 (v/v) containing 1% acetic acid, and then loaded onto a Sep-Pak® silica cartridge (500 mg; Waters). GAs were eluted with chloroform:ethyl acetate = 1:1 (v/v) containing 1% acetic acid and the elute was concentrated to dryness, dissolved in 50 µL of 20% methanol containing 0.05% acetic acid, filtered through a PTFE membrane, and then subjected to LC-MS/MS analysis. The LC-MS/MS system consisted of a Shimadzu Prominence 20A Series HPLC (Shimadzu, Kyoto, Japan) equipped with a 3200 QTRAP® LC-MS/MS System (AB Sciex, Framingham, MA, USA), using an electrospray ionization (ESI) interface. The purified samples were injected onto a Shim-pack XR-ODS column (2.2 µm, 75 × 2.0 mm; Shimadzu) at 45°C, and eluted at a flow rate of 0.2 mL·min⁻¹. Mobile phase A, consisting of water/methanol/acetic acid (80:19.95:0.05, v/v/v), and mobile phase B (methanol) were used for chromatographic separation. The initial condition was 100% A, which was maintained for 2 min, changing linearly to 40% A and 60% B after 5 min, and changing to 100% B after 10 min, and finally maintained at 100% B for 6 min. The column was equilibrated with the starting composition of the mobile phase for 12 min before each analytical run. Quantifica-

tion of the GAs was described previously (Fukuda et al., 2009).

Statistical analysis

Data were analyzed using a one-way ANOVA and the differences were contrasted using Tukey’s multiple comparison. All statistical analyses were performed at a significance level of *P*-value < 0.05 using R-3.2.0 (R Core Team, 2015).

Results

Isolation of CuGA20ox1 and CuGA20ox2 from Satsuma mandarin

To investigate the function of GA 20-oxidase genes in Satsuma mandarin, we isolated both cDNA and genomic DNA of these genes from Satsuma mandarin ‘Silverhill’ by polymerase chain reaction (PCR) with primer sets based on the sequences of *CcGA20ox1* (AJ250187) and *CcGA20ox2* (EU834066) (Huerta et al., 2009; Vidal et al., 2001). Coding sequences of *Citrus unshiu GA20ox1* (*CuGA20ox1*; Accession No. LC056054) and *Citrus unshiu GA20ox2* (*CuGA20ox2*; Accession No. LC056055) cDNA were 1152 and 1119 bp long including a stop codon and encoded 383 and 372 amino acids, respectively (Fig. 2A). Identities at the nucleotide level between *CuGA20ox1*

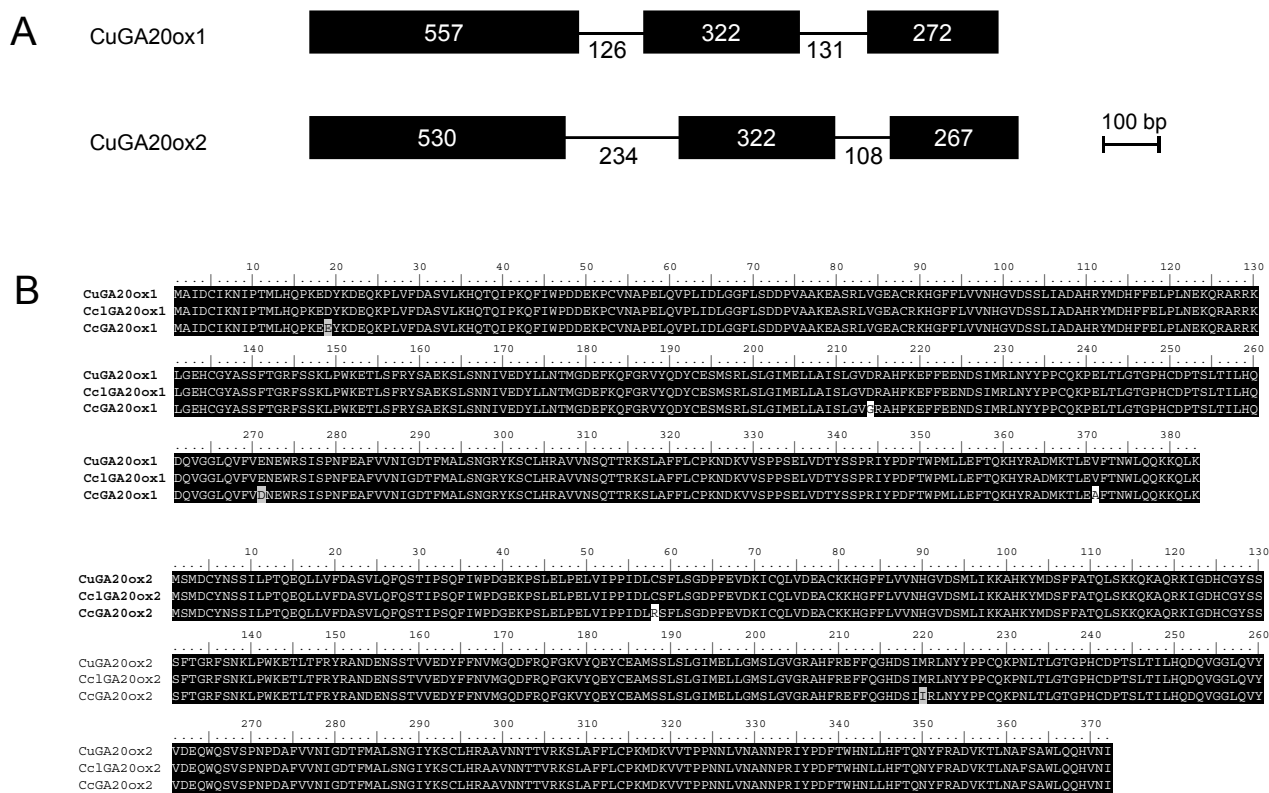


Fig. 2. Schematic representation of the genomic organization (A) and comparison of the deduced amino acid sequence (B) of *CuGA20ox1* and *CuGA20ox2*. Black boxes represent exons and lines represent introns. Numbers represent the lengths (bp) of exons (in the boxes) and introns (below the lines). The scale bar on the map represents approximately 100 bp.

and *CcGA20ox1* and between *CuGA20ox2* and *CcGA20ox2* were 99.5% and 99.4%, respectively, and those at the amino acid level were 99.0% and 99.2%, respectively (Fig. 2B). In addition, at the amino acid level, *CuGA20ox1* and *CuGA20ox2* were identical to *CclGA20ox1* (Ciclev10005157m) and *CclGA20ox2* (Ciclev10020694m) from Clementine, respectively. For genomic clones of *CuGA20ox1* and *CuGA20ox2*, sequences including the coding region of each gene and the exon-intron structure were identified (Fig. 2A). Southern blots of the genomic DNA of 12 *Citrus* species/cultivars and trifoliolate orange (*Poncirus trifoliata*) digested with *Xba*I hybridized with DIG-labeled cDNA of *CuGA20ox1* and *CuGA20ox2* showed a single band of about 10 kb for *CuGA20ox1* (Fig. 3A) and polymorphic bands for *CuGA20ox2* (Fig. 3B). To examine the evolutionary relationships among GA 20-oxidase genes including *CuGA20ox1* and *CuGA20ox2*, we performed phylogenetic analysis of the amino acid sequences corresponding to these genes from a variety of *Citrus* species and *Poncirus* sp. (Fig. 4A). Neighbor-joining (N-J) distance analysis generated an unrooted tree with four clades as previously shown by Huerta et al. (2009). *CuGA20ox1* and *CuGA20ox2* were classified into the different two clades as GA 20-oxidases from apple, common bean (*Phaseolus vulgaris*) and pea (*Pisum sativum*). Among *Citrus* species, putative GA 20-

oxidases from Satsuma mandarin were phylogenetically very similar or identical to those from sweet orange and Clementine as expected (Fig. 4B).

Organ-specific expression patterns of *CuGA20ox1* and *CuGA20ox2*

To identify the expression patterns of *CuGA20ox1* and *CuGA20ox2*, quantitative real-time reverse transcription-PCR (qRT-PCR) was performed on various tissues in Satsuma mandarin in juvenile and adult phases using primers specific to each gene (Table 1). The transcript of *CuGA20ox1* accumulated mainly in new (NL) and old (OL) leaves in both the juvenile and adult phases. It was also detected clearly in seeds and roots, stems, and nodes of seedlings in the juvenile phase and shoot apices (SA), juice sacs (JS) in November and December, and peels (PL) in December, but only faintly in flower buds (FB), young fruit (YF), and juice sacs and peels in September (Fig. 5A). In contrast, the transcript of *CuGA20ox2* accumulated specifically in flower buds with very low expression in peels (Fig. 5B).

Characteristics of transgenic *Arabidopsis* ectopically expressing *CuGA20ox1* or *CuGA20ox2*

To elucidate the function of GA 20-oxidase-like genes of Satsuma mandarin, *CuGA20ox1* and

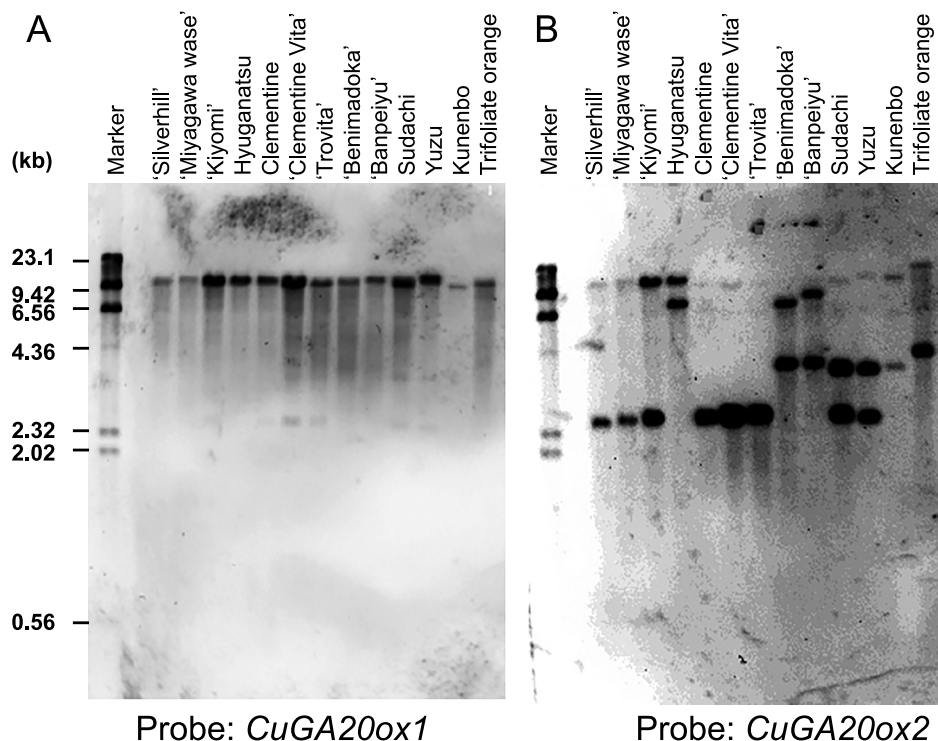


Fig. 3. Southern blot analysis of *CuGA20ox1* (A) and *CuGA20ox2* (B). The genomic DNA (5 μ g) of 'Silverhill' and 'Miyagawa-wase' Satsuma mandarin cultivars and other citrus/trifoliolate orange species/cultivars 'Kiyomi' tangor, Hyuganatsu, Clementine, 'Clementine Vita', 'Trovia' sweet orange, 'Benimadoka' and 'Banpeiyu' pummelo, Sudachi, Yuzu, Kunenbo, and trifoliolate orange were digested with *Xba*I, and then separated on a 0.8% agarose gel. DNA bands were transferred to Hybond N+ and hybridized with a digoxigenin (DIG)-labeled *CuGA20ox1* (A) or *CuGA20ox2* (B) cDNA coding region. Hybridization was performed in DIG Easy Hyb (Roche Diagnostics) at 42°C for 16 h followed by two washes in 0.5 \times SSC containing 0.1% (v/v) SDS at 68°C for 20 min. Molecular size markers are shown in kb on the left.

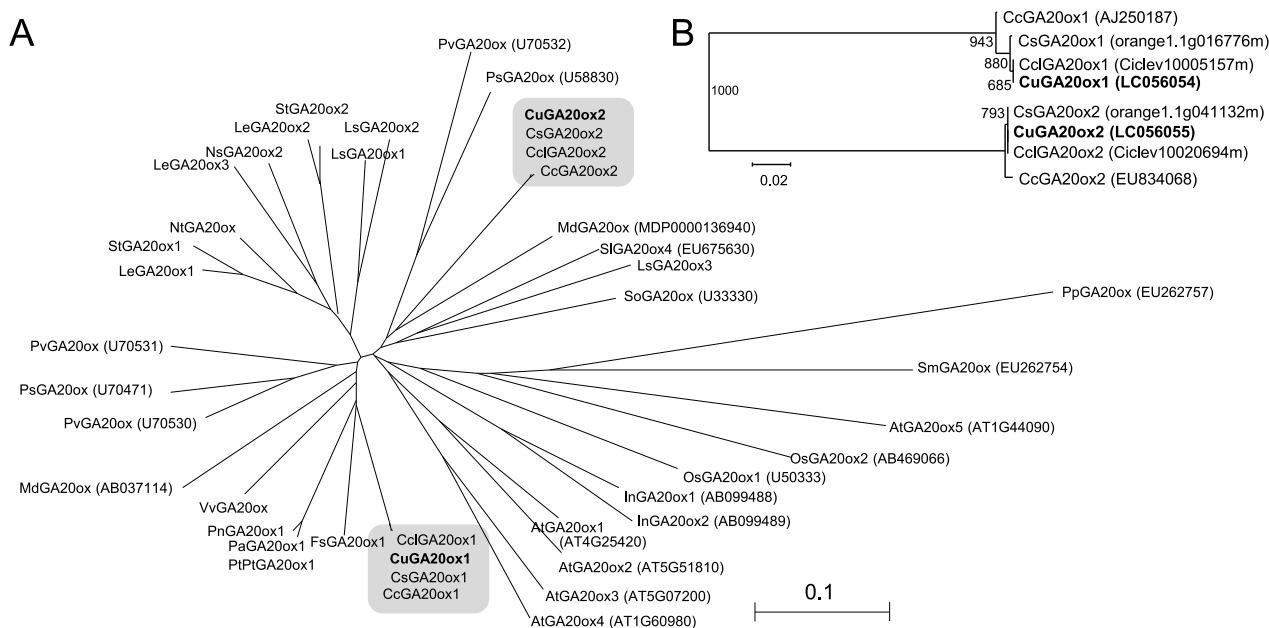


Fig. 4. Phylogenetic analysis of CuGA20ox1 and CuGA20ox2 together with other GA 20-oxidases. The tree was constructed by the neighbor-joining (N-J) method for the deduced amino acid sequence of the GA 20-oxidase genes from apple [*MdGA20ox* (AB037114), *MdGA20ox* (MDP0000136940)], *Arabidopsis* [*AtGA20ox1* (AT4G25420), *AtGA20ox2* (AT5G51810), *AtGA20ox3* (AT5G07200), *AtGA20ox4* (AT1G60980), *AtGA20ox5* (AT1G44090A)], Carrizo citrange [*CcGA20ox1* (AJ250187), *CcGA20ox2* (EU834068)], Clementine [*CclGA20ox1* (Ciclev10005157m), *CclGA20ox2* (Ciclev10020694m)], common bean [*PvGA20ox* (U70530, U70531, U70532)], European beech [*FsGA20ox1* (AJ420192)], grape [*VvGA20ox* (DQ508817)], lettuce [*LsGA20ox1* (AB012203), *LsGA20ox2* (AB012204), *LsGA20ox3* (AB031202)], morning glory [*InGA20ox1* (AB099488), *InGA20ox2* (AB099489)], pea [*PsGA20ox* (U70471), *PsGA20ox* (U58830)], *Physcomitrella patens* [*PpGA20ox* (EU262757)], poplar [*PnGA20ox1* (AB089675), *PaGA20ox1a* (AB090238), *PtPtGA20ox1* (AJ001326)], potato [*StGA20ox1* (AJ291453), *StGA20ox2* (AJ291454)], *Selaginella moellendorffii* [*SmGA20ox* (EU262754)], rice [*OsGA20ox1* (U50333), *OsGA20ox2* (AB469066)], Satsuma mandarin [*CuGA20ox1* (LC056054), *CuGA20ox2* (LC056055)], spinach [*SoGA20ox* (U33330)], sweet orange [*CsGA20ox1* (orange1.1g016776m), *CsGA20ox2* (orange1.1g041132m)], tobacco [*NtGA20ox* (AB012856), *NsGA20ox2* (AF494088)], and tomato [*LeGA20ox1* (AF049898), *LeGA20ox2* (AF049899), *LeGA20ox3* (AF049900), *SIGA20ox4* (EU675630)].

CuGA20ox2, we introduced the coding region of each gene under the control of the cauliflower mosaic virus (CaMV) 35S promoter fused with Ω sequence (35S Ω) into *Arabidopsis* (Fig. 6A). We analyzed five independent lines with 12–13 individuals ($n = 12–13$) in the T₂ generation for phenotypes including the numbers of days to flowering, the numbers of rosette and cauline leaves at flowering, and the numbers of inflorescences and lengths of first inflorescences one month after incubation (Fig. 6B; Table 2). For the numbers of days to flowering, rosette and cauline leaves, and inflorescences, there were no significant differences between transgenic lines with 35S Ω ::*CuGA20ox1* and 35S Ω ::*CuGA20ox2* and control plants [Wt (Col): wild-type plants; Vector/wt (Col): transgenic lines with an empty vector]. However, transgenic lines 1-1, 1-2, and 1-5 of 35S Ω ::*CuGA20ox1* with values of 23.19, 23.00, and 22.81 cm, respectively, and transgenic lines 2-1 and 2-3 of 35S Ω ::*CuGA20ox2* with values of 23.96 and 23.46 cm, respectively, showed statistically significant differences from wt (Col) and vector/wt (Col) with values of 13.21 and 17.35 cm, respectively in the length of the first inflorescences at the *P* value of 0.05, resulting in longer stems than those of control plants (Fig. 6B; Table 2).

In addition to the phenotypic analysis, the transgene expression in five independent lines per each construct was confirmed by qRT-PCR. From the transgenic lines with 35S Ω ::*CuGA20ox1*, lines 1-2 and 1-5 showed the highest expression, followed by lines 1-1, 1-3, and 1-4 in decreasing order (Fig. 7A). From the transgenic lines with 35S Ω ::*CuGA20ox2*, line 2-3 showed the highest expression, followed by lines 2-5, 2-1, 2-2, and 2-4 in decreasing order (Fig. 7B). As expected, the lines with relatively higher expression of each transgene, such as lines 1-1, 1-2, 1-5, 2-1, and 2-3 (indicated by asterisks in Figure 7), showed the phenotype of significantly elongated inflorescence, although line 2-5, which expressed *CuGA20ox2* at the same level as or slightly higher than line 2-1, did not show a significant difference in the length of the first inflorescence (Fig. 7B).

Effect of *CuGA20ox1* and *CuGA20ox2* on the level of gibberellins in transgenic *Arabidopsis*

In transgenic lines with 35S Ω ::*CuGA20ox1*, designated as line 1 in this experiment, GA₁₉ decreased, whereas both GA₂₉ and GA₈ increased significantly on the early-13-hydroxylation pathway (Fig. 8A, C, D). GA₂₀ tended to increase as compared with that in a wild-type control (Fig. 8B). On the non-13-

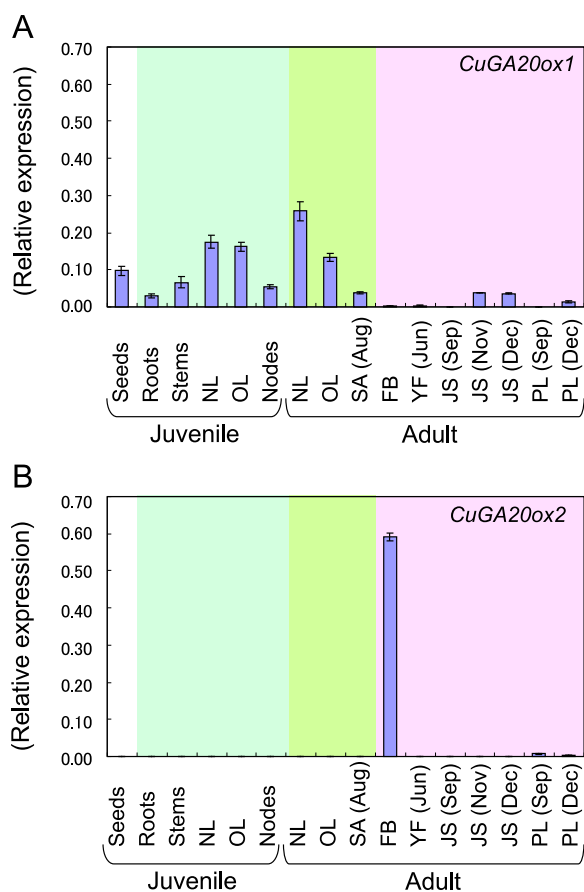


Fig. 5. Expression patterns of *CuGA20ox1* (A) and *CuGA20ox2* (B) in various Satsuma mandarin tissues by quantitative real-time RT-PCR. The samples for (A) and (B) from left to right are as follows: seeds, roots, stems, new leaves (NL), old leaves (OL), and nodes of two-year-old nucellar seedlings of a cultivar 'Silverhill' in the juvenile phase; NL, OL, and shoot apices (SA) in the adult phase; flower buds (FB), young fruit (YF) in June, juice sacs (JS) in September, November, and December, and peels (PL) in September and December in the reproductive phase. Levels of detected amplicons were normalized by reference to *CuActin* (*Citrus unshiu* actin gene). Values are means \pm SD of the results from three replicates. The primer sets used in this experiment and the PCR conditions are described in Table 1.

hydroxylation pathway in line 1, GA_{24} decreased, whereas GA_{34} increased significantly (Fig. 8E, H). In transgenic lines with 35S Ω ::*CuGA20ox2*, designated as line 2, GA_{20} increased significantly on the early-13-hydroxylation pathway (Fig. 8B). For other 13-OH GAs in line 2, changes in the levels of these GAs were not significantly different from those of the control. On the non-13-hydroxylation pathway in line 2, GA_{24} decreased, whereas GA_{34} increased significantly as in line 1 (Fig. 8E, H). GA_1 and GA_4 , important active GAs on the early-13-hydroxylation and non-13-hydroxylation pathways, respectively, could not be detected in lines 1 or 2 or in a wild-type control (data not shown).

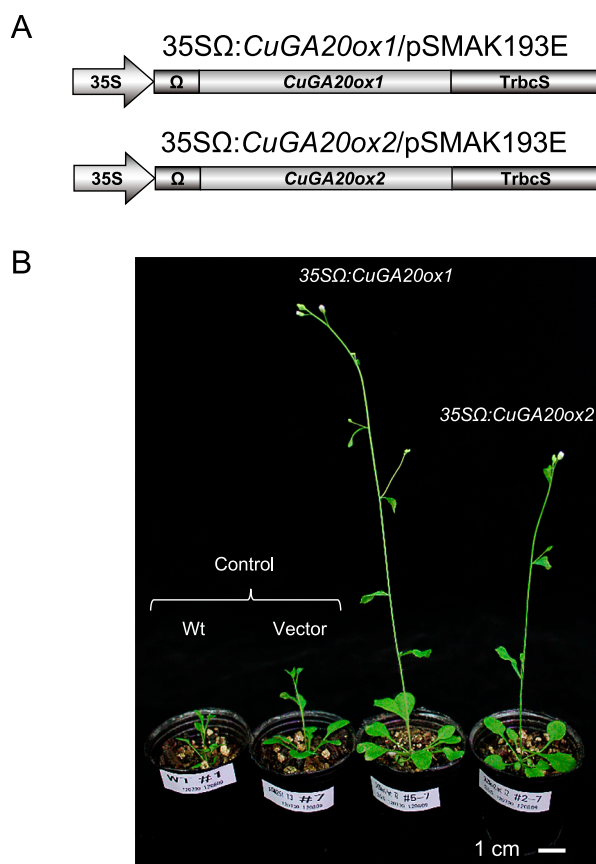


Fig. 6. Schematic representation of transformation vectors (A) and typical phenotypes of transgenic *Arabidopsis* with Satsuma mandarin *CuGA20ox1* (line1-5#7) and *CuGA20ox2* (line2-2#7) genes 24 days after incubation under long-day conditions. (B) Wt: wild-type plants; Vector: transgenic control plants with an empty vector.

Discussion

Satsuma mandarin has two GA 20-oxidase genes, *CuGA20ox1* and *CuGA20ox2*. The genomic sequence for *CuGA20ox1* is shorter than that for *CuGA20ox2*, although the coding region of cDNA for *CuGA20ox1* is slightly longer than that for *CuGA20ox2*, as Huerta et al. (2009) reported regarding two GA 20-oxidase genes in Carrizo citrange (Fig. 2). The amino acid sequence deduced from *CuGA20ox1* was identical to that in Clementine and very similar to that in Carrizo citrange and sweet orange; the amino acid sequence deduced from *CuGA20ox2* was identical to those in Clementine and sweet orange and very similar to that in Carrizo citrange (Figs. 2B and 4B). Southern blot analysis revealed that *Citrus* species/cultivars and trifoliolate orange have two types of GA 20-oxidase genes. Especially, the blot probed with *CuGA20ox2* showed polymorphic bands, indicating the diversity of citrus *GA20ox2* genes, although the blot probed with *CuGA20ox1* showed single bands at a similar molecular weight, indicating conserved sequences around the *Xba*I site in citrus *GA20ox1* genes. In considering

Table 2. Characteristics of transgenic lines ectopically expressing *CuGA20ox1* or *CuGA20ox2*.

Line	LD conditions (16-h light/8-h dark)					
	No. of plants	No. of days to flowering	No. of rosette leaves	No. of cauline leaves	No. of inflorescences	Length of 1st infl. (cm)
Wt (Col)	14	29.14±1.83 a	6.50±0.85 a	3.14±0.86 a	1.00±0.00 a	13.21±3.82 a
Vector/wt (Col)	14	27.54±1.71 abcd	7.00±1.00 a	3.85±1.07 abc	1.15±0.38 a	17.35±3.27 ab
35SΩ: <i>CuGA20ox1</i> /wt (T ₂)						
Line 1-1	13	25.23±2.24 d	6.77±1.30 a	3.69±0.75 abc	1.23±0.44 a	23.19±2.95 cd
Line 1-2	13	26.00±2.06 bcd	7.08±0.86 a	3.77±0.73 abc	1.23±0.44 a	23.00±3.50 cd
Line 1-3	13	27.46±3.57 abcd	7.77±1.79 a	3.46±0.78 ab	1.15±0.36 a	18.50±5.75 bc
Line 1-4	12	25.75±1.78 bcd	6.42±0.90 a	3.67±0.89 abc	1.33±0.49 a	21.63±4.24 bcd
Line 1-5	13	26.15±2.23 abcd	5.92±1.12 a	4.46±0.97 bc	1.00±1.00 a	22.81±4.23 cd
35SΩ: <i>CuGA20ox2</i> /wt (T ₂)						
Line 2-1	13	25.08±1.44 d	6.08±0.64 a	3.92±0.95 abc	1.15±0.38 a	23.96±2.45 d
Line 2-2	13	26.85±2.88 abcd	6.77±1.17 a	3.62±0.65 ab	1.08±0.28 a	19.58±3.09 bcd
Line 2-3	12	25.67±1.56 cd	6.58±0.90 a	4.75±0.75 c	1.08±0.29 a	23.46±2.62 d
Line 2-4	12	28.75±2.60 abc	5.75±0.62 a	2.83±0.83 a	1.17±0.39 a	16.75±1.74 ab
Line 2-5	12	28.92±3.65 ab	6.25±1.76 a	3.67±0.49 abc	1.08±0.29 a	16.71±2.90 ab

Plants in the second generation (T₂) and controls were grown under long-day (LD) conditions. Numbers of rosette and cauline leaves were counted on the day floral organs became visible. Numbers of inflorescences merging from the base were counted and length of 1st inflorescences (infl.) was measured one month after incubation. Values are means±standard deviation (SD). Tukey's multiple comparisons were performed to compare the effects of the ectopic expression of the genes. Superscripts letters indicate a statistically significant difference from results with other letters and values in bold indicate a statistically significance from those of controls in the same column ($P<0.05$).

the genealogy of Hyuganatsu it is interesting that Hyuganatsu has two bands—an upper band that is also seen in some mandarins and Yuzu and a lower band that is also seen in a pummelo cultivar ('Benimadoka'). The deduced amino acid sequences of *CuGA20ox1* and *CuGA20ox2* were identical to those of Clementine, confirming evolutionally close lineage between Satsuma mandarin and Clementine. Variation in the genome sequences of *CuGA20ox2* might explain the characteristics of flower and ovary development, which vary among species and cultivars in citrus.

CuGA20ox1 and *CuGA20ox2* were differentially expressed in various tissues as shown in Figure 5. *CuGA20ox1* was expressed in almost all of the tissues investigated, with relatively higher expression in vegetative than in reproductive tissues, whereas *CuGA20ox2* was specifically expressed in flower buds just before anthesis. These expression patterns were quite similar to those of *CcGA20ox1* and *CcGA20ox2* in Carrizo citrange (Huerta et al., 2009). The distinct expression patterns of *CuGA20ox1* and *CuGA20ox2* imply that the function of these two genes diverged in the process of evolution. *CuGA20ox1* was expressed in seeds but *CuGA20ox2* was not, suggesting that *CuGA20ox1* would regulate the basal level of active GAs in citrus seeds. On the other hand, *CuGA20ox2* was expressed specifically in flower buds, suggesting that it would be responsible for the level of active GAs, such as GA₁, GA₁₉, and GA₂₀, which are found in flower buds including ovaries at the early developmental stage or young fruit in Satsuma mandarin (Goto et al., 1989). The specific and relatively higher expression of *CuGA20ox2* in

flower buds would explain why GA-like activity is higher in Satsuma mandarin ovaries at anthesis (Takagi et al., 1989; Talon et al., 1990b) and why Satsuma mandarin show a higher rate of fruit growth than does Clementine at the early developmental stage around anthesis (Talon et al., 1990b). Gene expression of *CuGA20ox2* in reproductive organs of various species and cultivars remain to be investigated in detail.

Transgenic *Arabidopsis* plants ectopically expressing *CuGA20ox1* or *CuGA20ox2* were examined to elucidate the function of these two genes of Satsuma mandarin. Phenotypic analysis revealed that both *CuGA20ox1* and *CuGA20ox2* caused elongated inflorescence, but did not affect the timing of flowering in transgenic *Arabidopsis* as compared with wild-type controls (Fig. 6; Table 2). As expected, transgene expression in each line is positively related to the length of inflorescence, namely, the lines with relatively higher expression of *CuGA20ox1* or *CuGA20ox2* showed an elongated phenotype with a statistically significant difference except for line 2-5 (Fig. 7). Similar phenotypes were observed in transgenic *Arabidopsis* and tobacco plants ectopically expressing *AtGA20ox* and *CcGA20ox1*, respectively, which were taller and had larger inflorescences than those of control plants (Coles et al., 1999; Vidal et al., 2001).

CuGA20ox1 and *CuGA20ox2* in transgenic *Arabidopsis* functioned as *CcGA20ox1* in transgenic tobacco, therefore, the concentration of endogenous GAs was determined by using LC-MS/MS to clear the effect of these gene products on the GA biosynthetic pathways in transgenic *Arabidopsis*. Consistent with

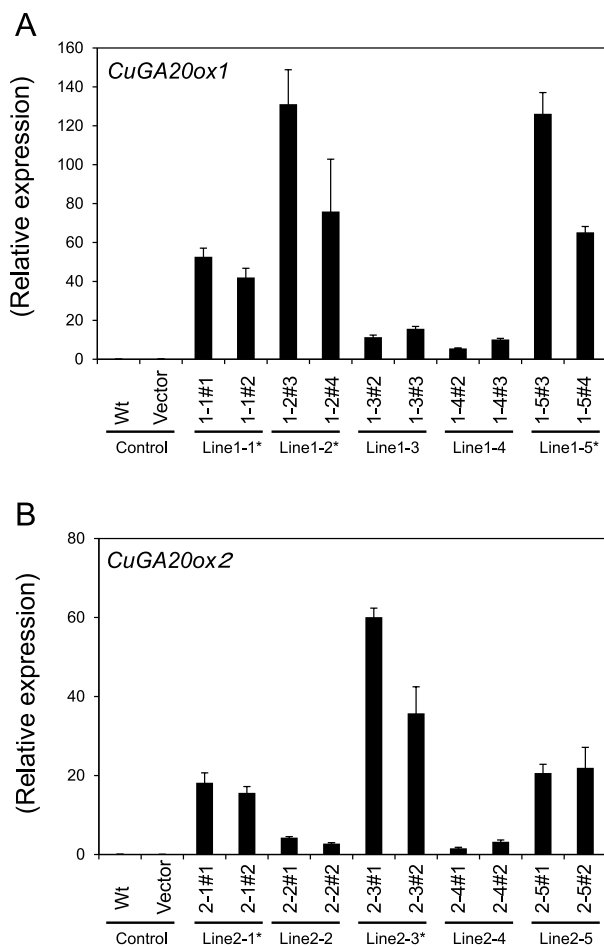


Fig. 7. Expression analysis for transgenes in whole plants of transgenic *Arabidopsis*. (A) Gene expression of *CuGA20ox1* in transgenic lines. (B) Gene expression of *CuGA20ox2* in transgenic lines. Levels of detected amplicons were normalized by reference to *CuActin*. Values are means \pm SD of the results from three replicates per line. Asterisks represent the lines that exhibit an elongated phenotype with a statistically significant difference from the wild-type controls shown in Table 2.

the fact that *Arabidopsis* mainly utilizes the non-13-hydroxylation pathway to accumulate active GAs such as GA₄, the concentrations of GA₉, GA₅₁, and GA₃₄ (Fig. 8F–H) are relatively higher on the non-13-hydroxylation pathway than are concentrations of GA₂₀, GA₂₉, and GA₈ (Fig. 8B–D), respectively, on the early-13-hydroxylation pathway, although the concentration of GA₂₄ (Fig. 8E) is lower than that of GA₁₉ (Fig. 8A) in the wild-type control. Active GA₁ and GA₄ could not be detected in this experiment likely because GAs were measured in two-month-old plants that were entering the stage of senescence, although Coles et al. (1999) detected both GA₁ and GA₄ in shoot tips of *Arabidopsis* plants about one month after sowing. Ectopic expression of *CuGA20ox1* and *CuGA20ox2* significantly affected the levels of GA₂₄ and GA₃₄ on the non-13-hydroxylation pathway; GA₂₄ decreased and GA₃₄ increased (Fig. 8E, H). This observation indicated that both *CuGA20ox1* and *CuGA20ox2* accelerated the

conversion of GA₂₄, a substrate of a GA 20-oxidase, to GA₉, a precursor of an active form of GA₄. In addition, an increased concentration of GA₃₄ suggested that most active GA₄ was converted to GA₃₄, an inactive metabolite of GAs, during two months of growing. Likewise, on the early-13-hydroxylation pathway, ectopic expression of *CuGA20ox1* significantly decreased GA₁₉ and increased GA₂₉ and GA₈, which were inactive metabolites of 2-hydroxylation of GA₂₀ and GA₁, respectively, suggesting the activation of this biosynthetic pathway (Fig. 8A, C, D). Fos et al. (2000) reported that unpollinated ovaries of a *pat-2* tomato mutant (Cuarenteno/*pat-2*) showing natural parthenocarpy contained less GA₁ and more GA₈ than those of wild type plants and also suggested that the content of GA₈ may be a measure of the previous GA₁ content because there was a correlation between the level of GA₈ produced from GA₂₀ and pea internode elongation (Ingram et al., 1986). *CuGA20ox2* also had a tendency to activate the early-13-hydroxylation pathway although it increased only GA₂₀ with a statistically significant difference (Fig. 8B). Taken together, we concluded that *CuGA20ox1* and/or *CuGA20ox2* activate both the early-13- and non-13-hydroxylation pathways, resulting in elongated inflorescences in transgenic *Arabidopsis*. *CcGA20ox1* was confirmed to encode for a GA 20-oxidase by utilizing the heterologous expression system in *Escherichia coli*, showing activities on both GA₁₂ and GA₅₃ as a substrate (Vidal et al., 2003); however, the expression product of *CcGA20ox2* catalyzed only the conversion of GA₁₂ to putative GA₉ (Huerta et al., 2009). How these two GA 20-oxidases regulate and coordinate the GA biosynthetic pathways in citrus must be studied to clarify more than a few physiological phenomena, such as flowering, fruit development and seedlessness, mediated by GA signal transduction.

Acknowledgements

We thank Dr. H. Ichikawa for providing the binary vector pSMK193E, Dr. E. E. Hood for providing *Agrobacterium tumefaciens* EHA101, and Ms. C. Hirano and Y. Uchida for their technical assistance.

Literature Cited

- Clough, S. J. and A. F. Bent. 1998. Floral dip: a simplified method for *Agrobacterium*-mediated transformation of *Arabidopsis thaliana*. *Plant J.* 16: 735–743.
- Coles, J. P., A. L. Phillips, S. J. Coker, R. Garcia-Lepe, M. J. Lewis and P. Hedden. 1999. Modification of gibberellin production and plant development in *Arabidopsis* by sense and antisense expression of gibberellin 20-oxidase genes. *Plant J.* 17: 547–556.
- Corey, E. J., R. L. Danheiser, S. Chandrasekaran, P. Siret, G. E. Keck and J. L. Gras. 1978. Stereospecific total synthesis of gibberellic acid. A key tricyclic intermediate. *J. Am. Chem. Soc.* 100: 8031–8034.
- Cross, B. E. 1960. Gibberellic Acid. Part XIII. The structure of ring A. *J. Chem. Soc.* 3022–3038.

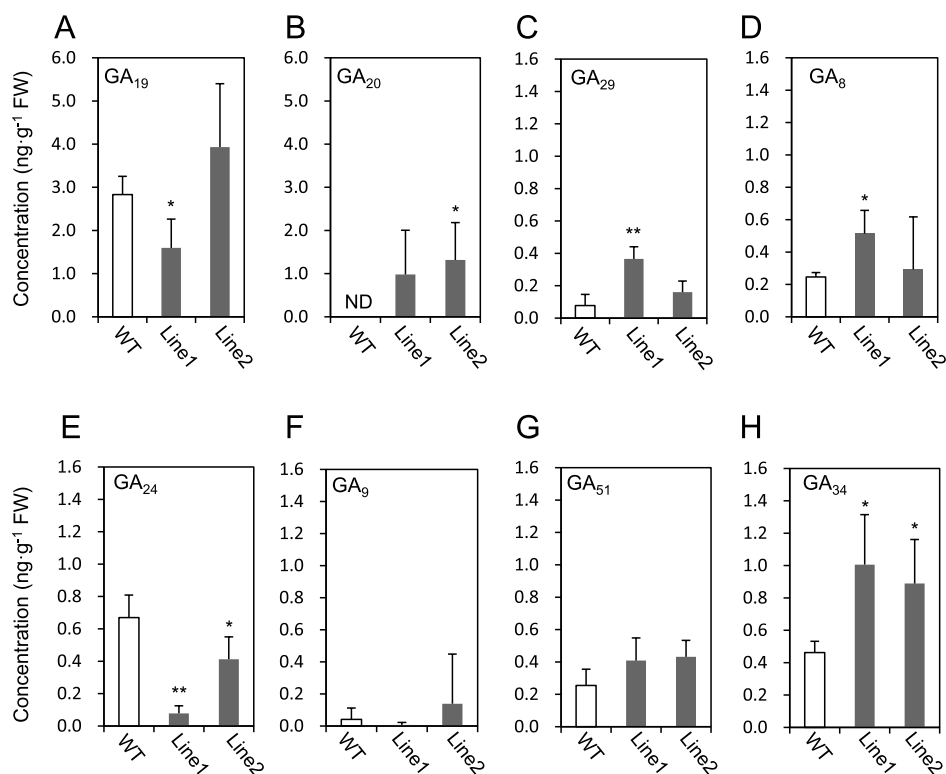


Fig. 8. Evaluation of eight GAs on both the early-13-hydroxylation and the non-13-hydroxylation pathways in transgenic *Arabidopsis*. (A–D) Concentrations of GA₁₉, GA₂₀, GA₂₄, and GA₈ on the early-13-hydroxylation pathway. (E–H) Concentrations of GA₂₄, GA₉, GA₅₁, and GA₃₄ on the non-13-hydroxylation pathway. Ten samples (one sample per each independent line of 35S::CuGA20ox1 or 35S::CuGA20ox2) were prepared and subjected to LC-MS/MS measurement in this experiment (n = 5, five biological replicates). Line 1 and line 2 represent transgenic lines with 35S::CuGA20ox1 and 35S::CuGA20ox2, respectively. Values are means ± SD. One or two asterisks indicate a statistically significant difference from the wild-type plants in the same column ($P < 0.05$, 0.01, respectively). ND, not detected.

Cross, B. E., J. F. Grove, J. MacMillan, J. S. Moffatt, T. P. C. Mulholland, J. C. Seaton and N. Sheppard. 1959. A revised structure for gibberellic acid. *Proc. Chem. Soc.* 302–303.

Fagoaga, C., F. R. Tadeo, D. J. Iglesias, L. Huerta, T. Lliso, A. M. Vidal, M. Talon, L. Navarro, J. L. García-Martínez and L. Peña. 2007. Engineering of gibberellin levels in citrus by sense and antisense overexpression of a GA 20-oxidase gene modifies plant architecture. *J. Exp. Bot.* 58: 1407–1420.

Fos, M., F. Nuez and J. L. García-Martínez. 2000. The gene pat-2, which induces natural parthenocarpy, alters the gibberellin content in unpollinated tomato ovaries. *Plant Physiol.* 122: 471–479.

Fukuda, M., S. Matsuo, K. Kikuchi, W. Mitsuhashi, T. Toyomasu and I. Honda. 2009. The endogenous level of GA₁ is upregulated by high temperature during stem elongation in lettuce through *LsGA3ox1* expression. *J. Plant Physiol.* 166: 2077–2084.

Goto, A., H. Yamane, N. Takahashi and K. Hirose. 1989. Identification of nine gibberellins from young fruit of Satsuma mandarin (*Citrus unshiu* Marc.). *Agric. Biol. Chem.* 53: 2817–2818.

Hedden, P. and Y. Kamiya. 1997. Gibberellin biosynthesis: enzymes, genes, and their regulation. *Ann. Rev. Plant Physiol. Plant Mol. Biol.* 48: 431–460.

Hedden, P. and A. L. Phillips. 2000. Gibberellin metabolism: new insights revealed by the genes. *Trends Plant Sci.* 5: 523–530.

Huerta, L., A. Garcia-Lor and J. L. Garcia-Martinez. 2009. Characterization of gibberellin 20-oxidases in the citrus hybrid Carrizo citrange. *Tree Physiol.* 29: 569–577.

Ikoma, Y., M. Yano, K. Ogawa, T. Yoshioka, Z. C. Xu, S. Hisada, M. Omura and T. Moriguchi. 1996. Isolation and evaluation of RNA from polysaccharide-rich tissues in fruit for quality by cDNA library construction and RT-PCR. *J. Japan. Soc. Hort. Sci.* 64: 809–814.

Ingram, T. J., J. B. Reid and J. MacMillan. 1986. The quantitative relationship between gibberellin A₁ and internode growth in *Pisum sativum* L. *Planta* 168: 414–420.

Iwamasa, M. 1966. Studies on the sterility in genus *Citrus* with special reference to the seedlessness. *Bull. Hort. Res. Sta. Japan Ser. (B)* 6: 1–81.

Jeanmougin, F., J. D. Thompson, M. Gouy, D. G. Higgins and T. J. Gibson. 1998. Multiple sequence alignment with Clustal X. *Trends Biochem. Sci.* 23: 403–405.

Kawarada, A. and Y. Sumiki. 1959. The occurrence of gibberellin A₁ in water sprouts of citrus. *Bull. Agr. Chem. Soc. Japan* 23: 343–344.

Kishi, T. and M. Tasaki. 1960. Budou ni taisuru Gibberellin riyou shiken [Dai ippou] Delaware ni tsuite. *Agric. Hort. (Nogyo-oyobi-Engei)* 35: 381–384 (In Japanese).

Kotoda, N., H. Hayashi, M. Suzuki, M. Igarashi, Y. Hatsuyama, S. Kidou, T. Igasaki, M. Nishiguchi, K. Yano, T. Shimizu, S. Takahashi, H. Iwanami, S. Moriya and K. Abe. 2010. Molecular characterization of *FLOWERING LOCUS T*-like genes of apple (*Malus × domestica* Borkh.). *Plant Cell Physiol.* 51: 561–575.

Kotoda, N., H. Iwanami, S. Takahashi and K. Abe. 2006. Antisense expression of *MdTFL1*, a *TFL1*-like gene, reduces the juvenile phase in apple. *J. Amer. Soc. Hort. Sci.* 131: 74–81.

- Kotoda, N., M. Wada, S. Kusaba, Y. Kano-Murakami, T. Masuda and J. Soejima. 2002. Overexpression of *MdMADS5*, an *APETALA1*-like gene of apple, causes early flowering in transgenic *Arabidopsis*. *Plant Sci.* 162: 679–687.
- Kurosawa, E. 1926. Ine bakanaebyoukin no bunpitsubutsu ni kansuru jikken kenkyu (Yohou). *Transactions of the Natural History Society of Taiwan* 16: 213–233 (In Japanese).
- Luckwill, L. C. and J. M. Silva. 1979. The effects of daminozide and gibberellic acid on flower initiation, growth and fruiting of apple cv Golden Delicious. *J. Hort. Sci.* 54: 217–223.
- Magome, H., T. Nomura, A. Hanada, N. Takeda-Kamiya, T. Ohnishi, Y. Shinma, T. Katsumata, H. Kawaide, Y. Kamiya and S. Yamaguchi. 2013. *CYP714B* and *CYP714B2* encode gibberellin 13-oxidases that reduce gibberellin activity in rice. *Proc. Natl. Acad. Sci. USA* 110: 1947–1952.
- Monselise, S. P. 1979. The use of growth regulators in citriculture; A review. *Sci. Hortic.* 11: 151–162.
- Mori, K., M. Shiozaki, N. Itaya, M. Matsui and Y. Sumiki. 1969. Synthesis of substances related to gibberellins—XXI: Total synthesis of (\pm)-gibberellins A₂, A₄, A₉, and A₁₀. *Tetrahedron* 25: 1293–1321.
- Nagao, A., S. Sasaki and R. P. Pharis. 1989. *Cryptomeria japonica*. p. 247–269. In: A. H. Halevy (ed.) *Handbook of flowering*. vol VI. CRC, Boca Raton, FL.
- Perrière, G. and M. Gouy. 1996. WWW-Query: An on-line retrieval system for biological sequence banks. *Biochimie* 78: 364–369.
- Poling, S. M. and V. P. Maier. 1988. Identification of endogenous gibberellins in Navel orange shoots. *Plant Physiol.* 88: 639–642.
- R Core Team. 2015. R: A language and environment for statistical computing. R Foundation for Statistical Computing, Vienna, Austria. URL <http://www.R-project.org/>.
- Takagi, T., A. Tomiyasu, M. Matsushima and T. Suzuki. 1989. Seasonal changes of GA-like substances in fruit and current shoots of Satsuma mandarin trees. *J. Japan. Soc. Hort. Sci.* 58: 569–573.
- Takahashi, N., Y. Hsu, H. Kitamura, K. Miyao, A. Kawarada, S. Tamura and Y. Sumiki. 1961. Biochemical studies on “Bakanae” fungus. *Agr. Biol. Chem.* 25: 860–869.
- Talon, M., P. Hedden and E. Primo-Millo. 1990a. Gibberellins in *Citrus sinensis*: A comparison between seeded and seedless varieties. *J. Plant Growth Regul.* 9: 201–206.
- Talon, M., L. Zacarias and E. Primo-Millo. 1990b. Hormonal changes associated with fruit set and development in mandarins differing in their parthenocarpic ability. *Physiol. Plant.* 79: 400–406.
- Talon, M., L. Zacarias and E. Primo-Millo. 1992. Gibberellins and parthenocarpic ability in developing ovaries of seedless mandarins. *Plant Physiol.* 99: 1575–1581.
- Tromp, J. 1982. Flower-bud formation in apple as affected by various gibberellins. *J. Hort. Sci.* 57: 277–282.
- Turnbull, C. G. N. 1989. Identification and quantitative analysis of gibberellins in *Citrus*. *J. Plant Growth Regul.* 8: 273–282.
- Vardi, A., I. Levin and M. Carmi. 2008. Induction of seedlessness in citrus: From classical techniques to emerging biotechnological approaches. *J. Amer. Soc. Hort. Sci.* 133: 117–126.
- Vidal, A. M., W. Ben-Cheikh, M. Talon and J. L. García-Martínez. 2003. Regulation of gibberellin 20-oxidase gene expression and gibberellin content in citrus by temperature and citrus exocortis viroid. *Planta* 217: 442–448.
- Vidal, A. M., C. Gisbert, M. Talon, E. Primo-Millo and I. Lopez-Díaz. 2001. The ectopic expression of a citrus gibberellin 20-oxidase enhances the non-13-hydroxylation pathway of gibberellin biosynthesis and induces an extremely elongated phenotype in tobacco. *Physiol. Plant.* 112: 251–260.
- Yabuta, T. and Y. Sumiki. 1938. Ine bakanaebyoukin no seikagaku. *Shokubutsu wo tochou seshimuru sayou aru busshitsu Gibberellin no kesshou ni tsuite*. *J. Agr. Chem. Soc. Japan* 14: 1526 (In Japanese).
- Yamaguchi, S. 2008. Gibberellin metabolism and its regulation. *Annu. Rev. Plant Biol.* 59: 225–251.